2023 8th International Conference on
Advanced Robotics and Mechatronics
July 8-10, Sanya, China

Experimental Characterization and Comparison of Three Typical Omnidirectional Mobile Robots

Zhuolun Li, Jiajun Long, Ximan Zhang, Chengyuan Gao, Shixing Jiang, Zheng Zhu, Zhenzhong Jia

2023 International Conference on Advanced Robotics and Mechatronics (ICARM) | 979-8-3503-0017-8/23/$31.00 ©2023 IEEE | DOI: 10.1109/ICARM58088.2023.10218777

***Abstract*— Omnidirectional vehicles (ODVs) or mobile robots are widely used in various industries due to their ability to move and rotate in narrow spaces without the need for multiple adjustments of moving direction or stopping. There are multiple types of ODVs, including those with standard wheels and those with special wheels such as Swedish wheels. Comprehensive characterization of the ODV's overall performance, which is very important when selecting specific configurations in the robot design process, is still missing in the literature. This paper qualitatively summarizes the comprehensive characteristics of three typical omnidirectional mobile robots in indoor scenarios through theoretical analysis and physical experiments. We compare the robot's performance through six representative evaluation metrics (maneuverability, efficiency, etc.) and express the results in a radar chart. The results of this study can assist designers in designing omnidirectional robots more effectively for specific application scenarios.**

I. Introduction

Mobile robots have become an indispensable part in many modern society applications, such as logistics [1], agriculture [2], military [3], medical [4], and rescue. In the research side, new designs of omnidirectional robots are constantly emerging [5]–[7], becoming one of the research hot topics in ground mobile robots. Compared to traditional non-omnidirectional robots, omnidirectional robots are usually more suitable for operations in small spaces because they can move more flexibly without the need of multiple turns. However, in the previous literature review [8], [9], the analysis of advantages and disadvantages of different omnidirectional robots was mainly based on the summary of the literature and the analysis of kinematic models, lacking direct comparisons of different types of omnidirectional robots. Selecting a suitable omnidirectional robot configuration is an important factor when designing and manufacturing omnidirectional robots. If different structures can be compared in multiple dimensions to highlight their characteristics in practical applications, it will bring more convenience to the design work.

The category of omnidirectional robots is diverse and can be divided into special wheeled and standard wheeled types based on the type of wheels used. The main types of special wheels are Mecanum [10], omniwheels [11], and ball wheels [12], among which Mecanum wheels are the most commonly used. Similar to traditional omni-directional wheels, Mecanum wheels consist of a series of freely rotating rollers connected to the outer edge of the wheel, but the rollers are oriented at a $45°$ angle to the wheel's central axis. A typical Mecanum robot often uses four Mecanum wheels, which are arranged in either an O-shaped or X-shaped configuration. However, some design features of Mecanum wheels can lead to negative effects such as vibration at high speeds and reduced control efficiency [13]. Standard wheeled robots mainly rely on caster wheels or active steering to achieve omnidirectional movements. Robots composed of independently steerable and independently driven wheel groups can achieve nonholonomic omnidirectional movement [6]. At least two wheel groups are required to achieve omnidirectional movement. Another commonly used method to achieve omnidirectional movement with traditional wheels is to construct wheels with offset steering axes. Robots that use the ASOC method belong to the holonomic omnidirectional robot category that uses traditional wheels.

The authors are with Shenzhen Key Laboratory of Biomimetic Robotics and Intelligent Systems; they are also with Guangdong Provincial Key Laboratory of Human-Augmentation and Rehabilitation Robotics in Universities, Department of Mechanical and Energy Engineering, Southern University of Science and Technology (SUSTech), Shenzhen, 518055, China.
Corresponding author: jiazz@sustech.edu.cn.
Video link: https://www.youtube.com/watch?v=re6EBwktieI

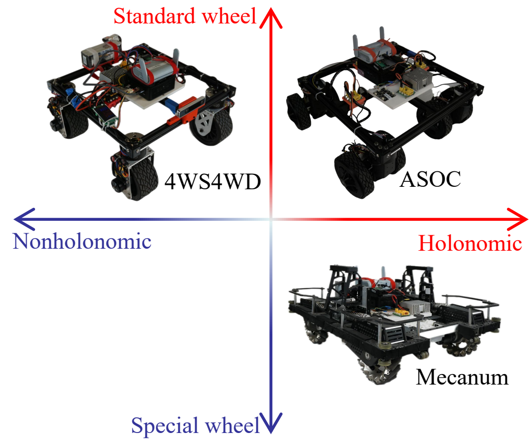

Fig. 1. The three omnidirectional robot platforms used in this paper are nonholonomic 4-wheel steering and 4-wheel drive (4WS4WD) robots that use traditional wheels, holonomic ASOC robots that use traditional wheels, and holonomic Mecanum robots that use special wheels.

Strictly speaking, holonomy is an essential attribute of omnidirectional robots. The motion of a holonomic mobile robot does not have kinematic constraints. However, nonholonomic pseudo-omnidirectional robots can also exhibit good omnidirectional motion performance in practical applications. Nonholonomic 4WS4WD mobile robots [14] need to rotate the steerable wheels to the corresponding positions before motion, and these types of omnidirectional robots are also called pseudo-omnidirectional robots. Usually, in scenarios with a main motion direction, pseudo-omnidirectional robots do not need to change the orientation of the wheels very quickly. There is no relevant research on the comparison of omnidirectional mobility performance between pseudo-omnidirectional robots and omnidirectional robots.

In theory, the rotational speed and translational speed of a robot are completely decoupled and independent. However, due to the motor speed limitations, there is an upper limit on the angular velocity of traction wheels. This leads to kinematic differences between different omnidirectional mobile robots [15]. Meanwhile, there are differences in traction and smoothness among the wheels of different configurations [16]. When performing agile maneuvers, these limitations significantly affect the actual motion performance of omnidirectional robots, making them difficult to meet the omnidirectional movement requirements. It is difficult to determine the robot's characteristics solely through the analysis of kinematics and dynamics without considering the characteristics of the tires.

This paper aims to verify the advantages and limitations of several typical omnidirectional mobile platforms (see Fig. 1) through actual experiments and to discuss their further improvements. These results can provide important references for the control and design of omnidirectional mobile robots. This article will first introduce the kinematic models of three typical omnidirectional mobile systems and the corresponding robots. Then, it will describe in detail the mobility tests and analyses of these three robots.

II. Platforms' Kinematics

It is a common practice to study omnidirectional moving systems using kinematic models. In this paper, three representative omnidirectional mobile systems are selected, namely: the holonomic omnidirectional mobile system with non-circular wheels, the holonomic omnidirectional mobile system with conventional wheels, and the nonholonomic pseudo-omnidirectional mobile system with conventional wheels. Furthermore, in the experimental section, the motion control of the three mobile platforms will be based on their corresponding kinematic models. The omnidirectional capability of these three types of mobile platforms has been proven by previous researchers, therefore the number of wheels for the omnidirectional mobile systems introduced in this section will be greater than the minimum required for achieving omnidirectional motion.

A. Mecanum Wheeled Robot Modeling

A single Mecanum wheel needs to be analyzed. The Mecanum wheel consists of a hub and a roller. Under the assumption of pure rolling motion, the total velocity can be decomposed into two components: one along the drive direction and the other along the slide direction. Motion direction is the non-sliding rolling direction of wheel i, which is in the same direction as the y_i axis of the reference coordinate system $\{B\}$, and it produces the driving speed. The sliding direction of the roller is the sliding direction. Its angle to the lateral are $\alpha_i = 45°, -45°, 45°, -45°$ for $i = 1, 2, 3, 4$ respectively, which generate sliding speed.

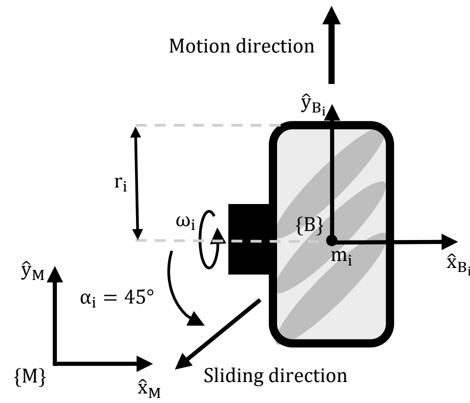

Fig. 2. Illustration of a single Mecanum wheel.

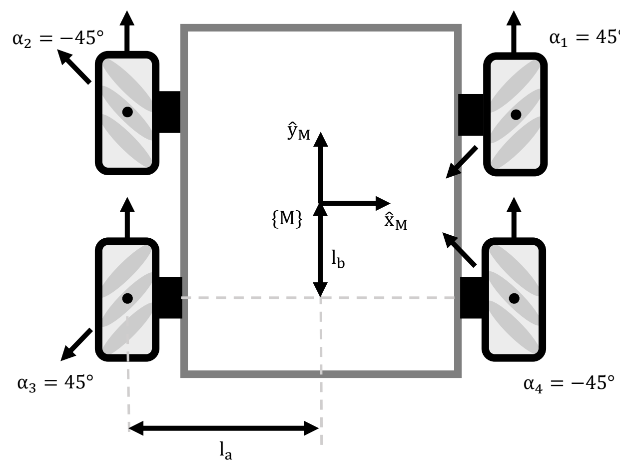

Fig. 3. Illustration of the whole Mecanum robot model.

After detailed force analysis, we can know that the linear speed of wheel i is the sum of motion speed and sliding speed. As shown in Fig.2, point m_i is the center of wheel i, and the linear velocity of point m_i can be obtained through body twist V_B which can be expressed as $V_B = [v_x \ v_y \ \omega]^T$ under the coordinate system $\{B\}$, it can be expressed as:

$$^{B}\dot{m}_i = \begin{bmatrix} 1 & 0 & -y_i \\ 0 & 1 & x_i \end{bmatrix} V_B \tag{1}$$

Through this variable, the linear velocity $^{d_i}\dot{m}_i$ in the driving direction can be calculated, this variable can be expressed as:

$$^{d_i}\dot{m}_i = \begin{bmatrix} 1 & t_{\alpha_i} \end{bmatrix} {}^{B}\dot{m}_i \tag{2}$$

The driving speed ω_i can be derived from the above two formulas:

$$\omega_i = \frac{1}{r_i} {}^{d_i}\dot{m}_i \tag{3}$$

So far, the velocity relationship between Mecanum wheels and the whole model has been obtained, as shown in Fig.3, and the kinematic model analysis has been completed.

B. 4WS4WD Mobile Robot Modeling

Then we will analyze the kinematic model of the 4WS4WD robot. Under this model, four wheels drive and

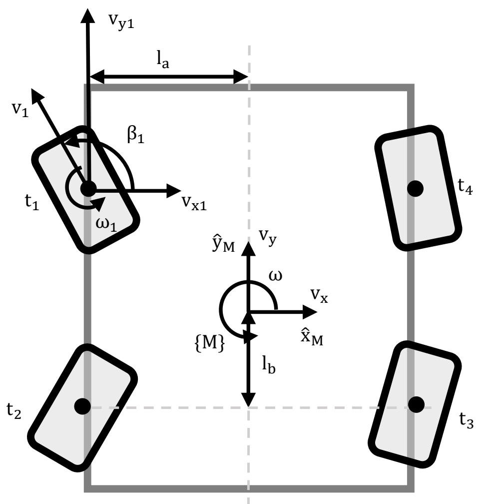

Fig. 4. Illustration of the whole 4WS4WD robot model.

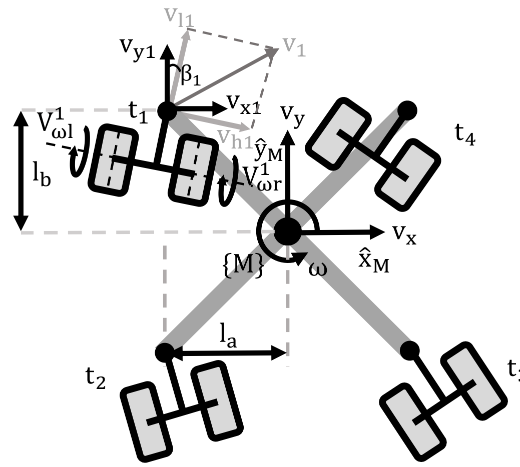

Fig. 5. Illustration of the whole ASOC robot model.

rotate independently, so each wheel needs to be analyzed independently. Here, we select one single wheel shown in the figure for analysis. First, through the calibration of the main coordinate system and the wheel coordinate system, the center of mass of the four wheels can be obtained, they are $(x_1, y_1) = (-l_a, l_b)$; $(x_2, y_2) = (-l_a, -l_b)$; $(x_3, y_3) = (l_a, -l_b)$; $(x_4, y_4) = (l_a, l_b)$. We need to define some characters in Fig.4. The linear speed of the entire model is v, and for each wheel i, its speed is v_i, which can be expressed as:

$$v = \sqrt{v_x^2 + v_y^2}; v_i = \sqrt{v_{x_i}^2 + v_{y_i}^2} \tag{4}$$

And ω is the angular velocity of the entire model. The equation below is under the assumption of no slipping situation, the speed relationship between the 4WS4WD model and each wheel can be obtained. So derive the wheel t_i, which can be expressed as:

$$\begin{bmatrix} v_{x_i} \\ v_{y_i} \end{bmatrix} = \begin{bmatrix} 1 & 0 & -y_i \\ 0 & 1 & x_i \end{bmatrix} \begin{bmatrix} v_x \\ v_y \\ \omega \end{bmatrix} \tag{5}$$

and $\beta_i = atan(v_{y_i}/v_{x_i})$.

So far, the velocity relationship between 4WS4WD wheels and the whole model has been obtained, and the kinematic model analysis has been completed.

C. ASOC-based Mobile Robot Modeling

The following is the kinematic analysis of the ASOC wheel model. In this model, eight wheels rotate independently, controlled by eight motors, and each motor in $t_i$prevents excessive wheel rotation. $\{M\}$ is the model coordinate system of ASOC wheel model, and v_x and v_y are the velocities in the direction of model x and y respectively. The resultant velocity is $v = \sqrt{v_x^2 + v_y^2}$, where ω is the total angular velocity of the ASOC wheel model. t_i is selected for analysis, as shown in Fig.5, v_i is the resultant speed of left and right wheels in the coordinate system t_i, which can be expressed as:

$$v_i = \sqrt{v_{l_i}^2 + v_{h_i}^2} = \sqrt{v_{x_i}^2 + v_{y_i}^2} \tag{6}$$

where v_{x_i} and v_{y_i} are the velocities of the pivot point of the ASOC module in the direction of x and y, respectively. And v_{l_i} and v_{h-I} are the velocities in the direction of x and y in the coordinate system of t_i, respectively. Next, take a look at the other parameters in the figure below, β_i is the angle between the coordinate system of $\{M\}$ and t_i. $V^i_{\omega l}$ and $V^i_{\omega r}$ are the velocities of the left wheel and the right wheel in the ASOC module of t_i, respectively. x_i and y_i are the x and y wheelbase departures from the pivot point of each ASOC module to the model coordinate system, respectively. At any moment of model movement, its subject can be regarded as a rigid body. After the parameters are basically defined, according to the structure of ASOC wheel model, the left wheel and right wheel speed of t_i module can be calculated, which can be expressed as:

$$\begin{bmatrix} V^i_{\omega_l} \\ V^i_{\omega_r} \end{bmatrix} = C_{\omega i} R_i C_i \begin{bmatrix} v_x \\ v_y \\ \omega \end{bmatrix} \tag{7}$$

where

$$C_i = \begin{bmatrix} 1 & 0 & -y_i \\ 0 & 1 & x_i \end{bmatrix} \text{is the speed transition,} \tag{8}$$

$$R_i = \begin{bmatrix} \cos\beta_i & -\sin\beta_i \\ \sin\beta_i & \cos\beta_i \end{bmatrix} \text{is the rotation matrix,} \tag{9}$$

$$C_{\omega i} = \frac{1}{R} \begin{bmatrix} \frac{L_s}{2L_o} & 1 \\ -\frac{L_s}{2L_o} & 1 \end{bmatrix} \text{is the Jacobian matrix.} \tag{10}$$

In the Jacobian matrix, R is the radius of the wheel, L_s is the offset distance of the wheel, and L_o is the distance between the hub shaft and the wheel's center of mass. So far, the velocity relationship between ASOC wheels and the whole model has been obtained, and the kinematic model analysis has been completed.

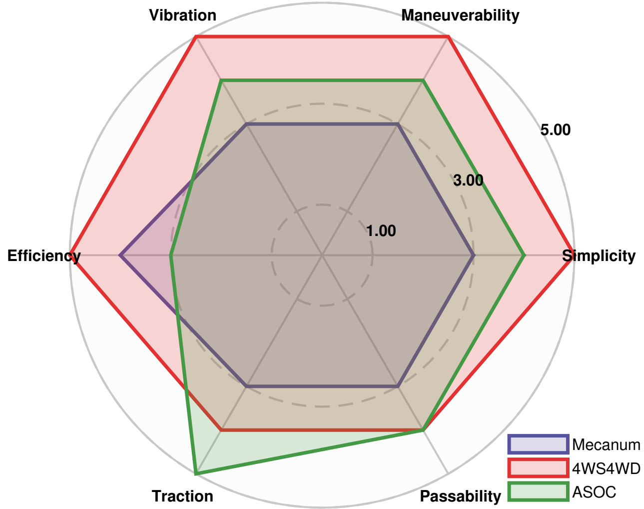

Fig. 6. A radar chart is obtained by comparing the relative performance of different entities. The robot with the best performance in a certain dimension is given a score of 5, while the worst performer is given a score of 3.

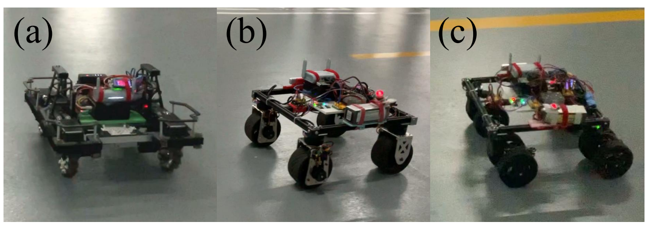

Fig. 7. The three robot platforms that participated in experiments are shown in the figures. Figure (a) shows the Mecanum robot, Figure (b) shows the 4WS4WD robot and Figure (c) shows the ASOC robot. The testing environment is an indoor parking lot with a wear-resistant epoxy material on the ground.

III. Evaluation

In order to evaluate the three types of omnidirectional robots mentioned in this paper from multiple dimensions, we adopted the method of practical experiments and comparison. The three robots are the four-wheeled Mecanum robot, the 4WS4WD robot, and the ASOC robot (see Fig. 7). According to the previous literature summary, this section evaluates omnidirectional robots from structural complexity, maneuverability, and efficiency [2], [15], [16]. The vibration [17], traction capacity [15], and passability [5] of these three types of robots have been discussed in previous studies, and therefore will not be reiterated in this section.

In Fig. 6, the numerical values of various performance indicators are obtained through comparison. For a particular characteristic, the robot with the weakest performance scored 3 points, and the robot with the best performance scored 5 points. If the performance is close or equal, it is scored the same. The specific evaluation content of the relevant characteristics will be discussed in detail in Sec. III-A and III-B. The results of several dimensions of evaluation are presented below. In terms of traction ability, the ASOC robot has more driving motors (8 motors) and uses traditional wheels, while the Mecanum robot uses only 4 motors, and the rotational efficiency of Mecanum wheels is lower than that of traditional wheels [16]. Therefore, the ASOC robot has the most potent traction ability, while the Mecanum wheel has the weakest traction ability. In terms of vibration, the multi-roller structure used by the Mecanum wheel will produce discontinuous contact during movement [17], causing significant vibration. The ASOC robot uses 8 motors, resulting in more vibration than the 4WS4WD robot. In terms of passability, the Mecanum wheel has weak passability during lateral movement. The ASOC robot and the 4WS4WD robot, both using traditional wheels, have similar passability. In terms of structural complexity, the Mecanum wheel has the most number of parts, mainly due to the complex structure of the roller-combined wheel. The ASOC wheel group has two motors, which increases the complexity of the structure, while the 4WS4WD robot is the most concise among the three robots. In terms of maneuverability, based on the experiments in Sec. III-A and III-B, it can be seen that the 4WS4WD robot performs the best in terms of maneuverability, while the overall performance of the Mecanum robot is the worst. In terms of power consumption and efficiency, based on the experimental results, the ASOC robot has more driving motors, resulting in the highest energy consumption when completing the same working conditions, and the lowest driving efficiency. The mecanum robot has a lower driving efficiency due to significant slippage at high speeds. In comparison, the 4WS4WD robot has the lowest energy consumption.

The experimental results will have performance deviations caused by vehicle size and part selection. In order to reflect the impact of robot configuration on practical applications, the wheel sets of these three omnidirectional robot platforms are directly rigidly connected to the body. And uniformly adopt the four-wheel set platform, because the four-wheel set is the most widely used in various fields. Table I is the parameter table of the three robots. To compare the motion performance between platforms, we standardized the platform frame, motor selection, and tire selection (each wheel group has the same tire width). The weight difference between the platforms is mainly due to the different number of actuators used, which is caused by the choice of robot type. In order to compare the assembly complexity of each platform, the table also counts the number of parts (including fasteners) for each robot.

We use the Intel T265 visual odometry as the trajectory recording module, which can ensure a certain positioning accuracy (1cm) indoors. The path tracking module adopts a forward-looking PI controller. Under different target speed

TABLE I

The parameter table of the three robots.

	Mecanum	**4WS4WD**	**ASOC**
Length (m)	0.370	0.385	0.385
Width (m)	0.315	0.385	0.385
Actuators	4 * M3508	4*M3508 4*GM6020	8*M3508
Weight (kg)	9.2	8.0	10.9
Parts (pcs)	708	228	236

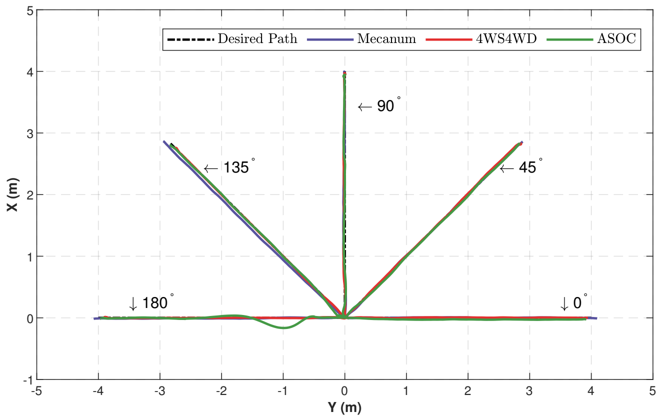

Fig. 8. In isotropic experiments, the motion trajectory diagrams of three robots are presented. The tracking errors of Mecanum and 4WS4WD robots are similar, while the ASOC robot exhibits significant oscillations during the initial motion in large turning scenarios. However, its tracking error converges within 3 meters.

conditions, only the target speed of the control module is changed, and the parameters in the PI controller are not modified.

A. Characterization of the System's Kinematic Isotropy

From the kinematic analysis of omnidirectional robots, they should have the same ability to move in all directions, but the dynamics of the robot, the dynamics of the wheel-set, and the slip of the tires will cause deviations in actual motion. In order to study the influence of configuration on motion performance in all-directional motion, we designed isotropic experiments (see Fig. 8). The platform is moved in various directions (0°, 45°, 90°, 135°, 180°) at a target speed of $1m/s$ to evaluate the tracking error and speed maintenance ability of the robot.

As shown in Fig. 9(a-c), Mecanum and 4WS4WD robots are capable of maintaining very low tracking errors in all directions (maximum tracking error $< 0.07m$). ASOC robot exhibits a significant increase in maximum tracking error ($> 0.15m$) in motions greater than 90°. The Mecanum robot has different resistances in omnidirectional motion, which makes it difficult to maintain target speed in all directions (see Fig. 9(a)). The average power consumption of the Mecanum robot (see Fig. 9(e)) in all directions can also demonstrate its issues with maintaining speed. The average driving power consumption of the robot is greater than $15W$ at 45°, 90°, and 135° (higher than at 0° and 180°), and the robot cannot reach the predetermined speed, resulting in steady-state speed tracking errors. Literature also indicates that omnidirectional robots with non-circular wheels are more susceptible to performance losses due to installation errors [16].

The 4WS4WD robot has a wheel steering time. As the motion angle increases, the influence of the steering time on the actual motion speed also increases (see Fig. 9(b)). It is worth noting that the torque of the steering motor needs to overcome the scrubbing torque of the tires when turning in place. In practical applications, when the chassis is under high load, there will be a significant increase in the response time of the steering motor to reach the target position.

The ASOC robot experiences significant speed fluctuations in motions greater than 90 degrees due to the slow speed of the wheel set transition. In the 180° scenario, this transition process takes nearly 1 second, during which the ASOC robot experiences significant tracking errors (see Fig. 9(c)).

The power consumption of the 4WS4WD and ASOC robots is relatively similar in omnidirectional motion. The ASOC robot exhibits the highest power consumption. Due to the use of fewer actuators, the Mecanum robot has the lowest average power consumption (see Fig. 9(e)). Overall, the 4WS4WD robot exhibits the best performance in kinematic isotropy, while the Mecanum robot has good path tracking ability but has issues with maintaining speed. The ASOC robot performs poorly in scenarios involving large turning angles.

B. Path Following

The reference path used for evaluation is a continuous but non-differentiable path. The robot needs to go through four 90-degree corners in succession (see Fig.10(a-i) and (b-i)). This path not only demonstrates the omnidirectional movement characteristics of the robot, but also evaluates the limitations of the three types of robots. The experiments were performed on a flat indoor terrain. The target velocities are 0.5 m/s, 1.0 m/s, 1.5 m/s, 2.0 m/s, and 2.5 m/s.

From the average error and standard deviation graphs at various speeds (Fig. 10(c)), it can be observed that increasing the target speed exponentially increases the average and standard deviation of tracking errors. Tagliavini et al. [15] proposed using kinematics-based velocity space under wheel speed constraints as an indicator for evaluating omnidirectional robots. However, in practical experiments, due to the limited adhesion provided by the tires, there are significant differences in the motion capabilities of each robot before approaching the wheel speed limit. Next, two scenarios with relatively low speed of 1.0m/s and relatively high speed of 2.0m/s are selected for analysis. At a speed of 1.0m/s (see Fig.10(a)), the tracking performance of all three platforms is good, with the 4WS4WD robot exhibiting the smallest oscillation at the turning position. During the rapid change of direction of the ASOC robot's wheel group, the orientation of the ASOC robot changed significantly. The speed tracking of the three platforms was not significantly affected by the turning angle. At a speed of 2.0m/s (see Fig.10(b)), it can be seen from the speed change graph of the three robots during tracking that even when running at high speeds, the omnidirectional robot's overall speed does not completely stop when tracking non-differentiable trajectories. From the trajectory, Mecanum has the largest deviation at corners and the longest recovery time. The 4WS4WD robot experiences significant speed loss after turning (see Fig. 10(b-iii)). Under low-speed conditions (0.5m/s and 1.0m/s), the Mecanum robot have the lowest energy consumption. However, at higher speeds, the Mecanum robot doesn't have an efficiency advantage. Compared to the Mecanum and ASOC robot,

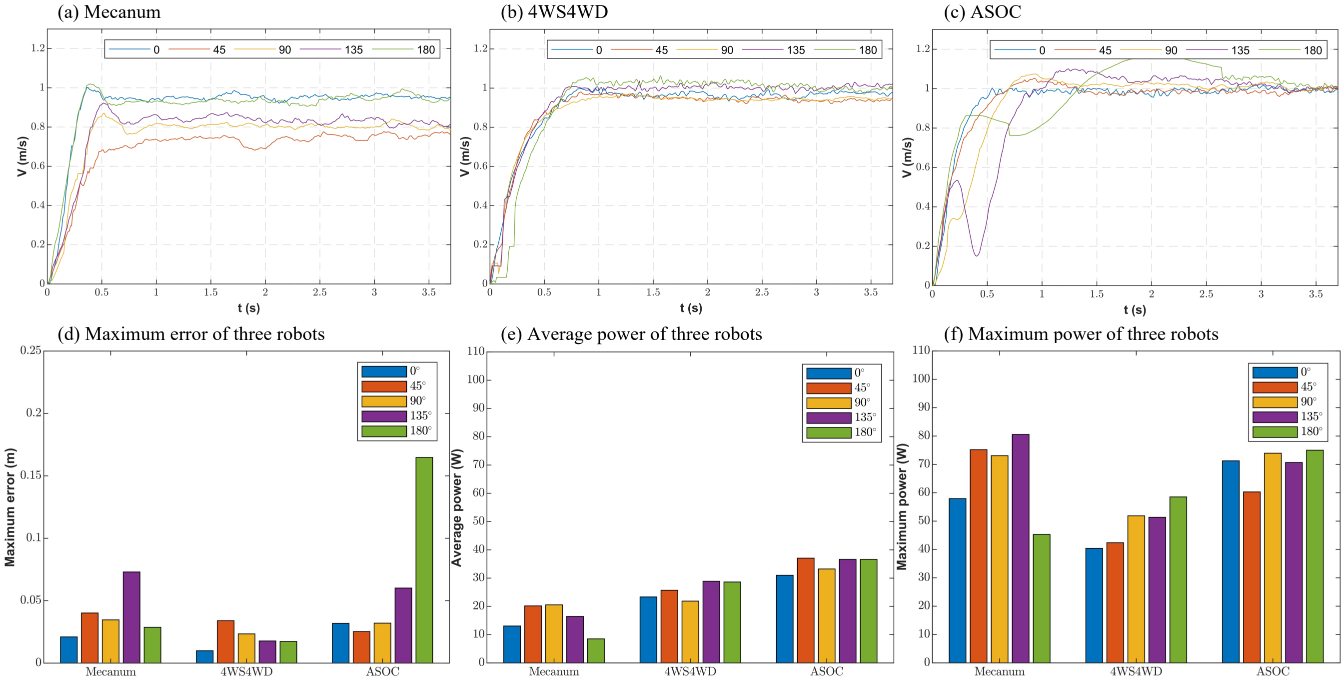

Fig. 9. Figure (a-c) show the variation of motion speed over time for three robots in isotropic experiments. The tracking errors of the Mecanum and 4WS4WD robots are close, while the ASOC robot exhibits significant oscillations during initial motion in large turning scenarios, but eventually converges within 3 meters of tracking error. Figure (d) displays the maximum error of the three platforms. Figure (e) displays the average power consumption of the three platforms. Figure (f) displays the maximum power consumption of the three platforms.

the 4WS4WD robot performs the best under high-speed conditions, with the lowest power consumption and tracking error (see Fig. 10(e)) . Since the wheels of the ASOC are driven independently by 8 motors, the ASOC robot has a higher power output limit at high speeds (see Fig. 10(f)) and can maintain a higher speed when turning.

IV. Conclusion

This paper employs experimental and comparative methods to study the comprehensive characteristics of different configurations of omnidirectional robots. Based on two dimensions, namely the configuration of the wheels and the platform's motion characteristics, we classify existing omnidirectional robots into four categories. We then build three representative platforms. In order to improve the reliability of the test results, multiple variables are standardized in the design of these robots, and forward kinematics is used for joint velocity control. In the isotropic experiments, we found that holonomic omnidirectional robots exhibit anisotropic motion effects due to their configuration characteristics and installation accuracy. The 4WS4WD omnidirectional robot exhibits excellent isotropic motion effects when it can turn quickly. In the path tracking experiments, all three types of omnidirectional robots can maintain low tracking errors under low-speed conditions. However, due to the limited adhesion provided by the wheels, the robots cannot maintain low tracking errors when changing path at high speeds. As the target speed increases, the tracking error increases exponentially. The adhesion coefficient of special wheels is usually lower than that of traditional wheels, resulting in poorer path tracking capabilities. This paper summarizes the performance differences of different types of omnidirectional robots in different dimensions, which can provide convenience for the selection of omnidirectional robot designs. The main argument of this paper is based on qualitative analysis, while not taking into account the effects of unified variables (load, size, etc.) on different types of robots. In the future, there are plans to use quantitative analysis to evaluate the comprehensive performance of omnidirectional robots.

Acknowledgment

This work was supported in part by the Science, Technology and Innovation Commission of Shenzhen Municipality under Grant No.ZDSYS20200811143601004.

References

[1] C. Sprunk, B. Lau, P. Pfaff, and W. Burgard, "An accurate and efficient navigation system for omnidirectional robots in industrial environments," *Autonomous Robots*, vol. 41, pp. 473–493, 2017.

[2] X. Gao, J. Li, L. Fan, Q. Zhou, K. Yin, J. Wang, C. Song, L. Huang, and Z. Wang, "Review of wheeled mobile robots' navigation problems and application prospects in agriculture," *IEEE Access*, vol. 6, pp. 49 248–49 268, 2018.

[3] G. Witus, "Mobility potential of a robotic six-wheeled omnidirectional drive vehicle (odv) with z-axis and tire inflation control," in *Unmanned Ground Vehicle Technology II*, vol. 4024. SPIE, 2000, pp. 106–114.

[4] G.-Z. Yang, B. J. Nelson, R. R. Murphy, H. Choset, H. Christensen, S. H. Collins, P. Dario, K. Goldberg, K. Ikuta, N. Jacobstein *et al.*, "Combating covid-19—the role of robotics in managing public health and infectious diseases," p. eabb5589, 2020.

[5] S. Jiang, Z. Li, S. Lin, W. Shi, Z. Zhu, H. Che, S. Yin, C. Zhang, and Z. Jia, "Design, control and experiments of an agile omnidirectional mobile robot with active suspension," in *2022 IEEE 18th International Conference on Automation Science and Engineering (CASE)*. IEEE, 2022, pp. 913–918.

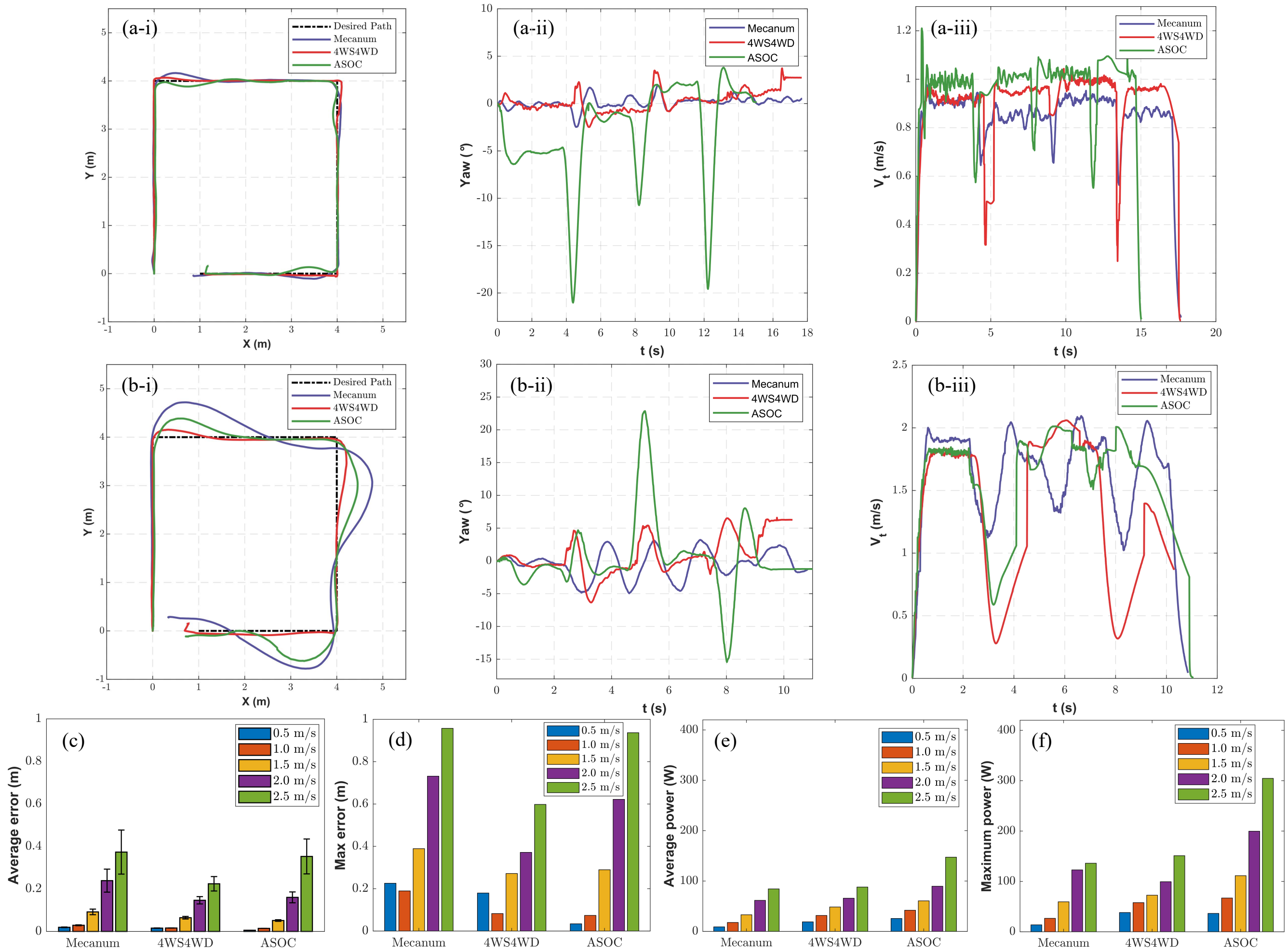

Fig. 10. Figure(a) shows the results of the three robots operating at a speed of 1.0m/s. Figure (a-i) shows the trajectory, Figure (a-ii) shows the yaw angle variation over time, and Figure (a-iii) shows the speed variation over time. Figure(b) shows the results of the three robots operating at a speed of 2.0m/s. Figure (b-i) shows the trajectory, Figure (b-ii) shows the yaw angle variation over time, and Figure (b-iii) shows the speed variation over time. Figure (c) shows the average error and standard deviation of the three robots at various speeds. Figure (d) shows the maximum error of the three robots at various speeds. Figure (e) shows the average power consumption of the three robots at various speeds. Figure (f) shows the maximum power consumption of the three robots at various speeds.

[6] F. Ferland, L. Clavien, J. Frémy, D. Létourneau, F. Michaud, and M. Lauria, "Teleoperation of azimut-3, an omnidirectional non-holonomic platform with steerable wheels," in *2010 IEEE/RSJ International Conference on Intelligent Robots and Systems*. IEEE, 2010, pp. 2515–2516.

[7] G. Runge, G. Borchert, P. Henke, and A. Raatz, "Design and testing of a 2-dof ball drive: An omnidirectional wheel for mobile robots," *Journal of Intelligent & Robotic Systems*, vol. 81, pp. 195–213, 2016.

[8] F. Rubio, F. Valero, and C. Llopis-Albert, "A review of mobile robots: Concepts, methods, theoretical framework, and applications," *International Journal of Advanced Robotic Systems*, vol. 16, no. 2, p. 1729881419839596, 2019. [Online]. Available: https://doi.org/10.1177/1729881419839596

[9] G. Campion, G. Bastin, and B. Dandrea-Novel, "Structural properties and classification of kinematic and dynamic models of wheeled mobile robots," *IEEE transactions on robotics and automation*, vol. 12, no. 1, pp. 47–62, 1996.

[10] H. Taheri, B. Qiao, and N. Ghaeminezhad, "Kinematic model of a four mecanum wheeled mobile robot," *International journal of computer applications*, vol. 113, no. 3, pp. 6–9, 2015.

[11] C.-W. Wu and C.-K. Hwang, "A novel spherical wheel driven by omni wheels," in *2008 International Conference on Machine Learning and Cybernetics*, vol. 7. IEEE, 2008, pp. 3800–3803.

[12] M. West and H. Asada, "Design of ball wheel mechanisms for omnidirectional vehicles with full mobility and invariant kinematics," 1997.

[13] B. Adamov, "Influence of mecanum wheels construction on accuracy of the omnidirectional platform navigation (on exanple of kuka youbot robot)," in *2018 25th Saint Petersburg International Conference on Integrated Navigation Systems (ICINS)*. IEEE, 2018, pp. 1–4.

[14] M.-H. Lee and T.-H. S. Li, "Kinematics, dynamics and control design of 4wis4wid mobile robots," *The Journal of Engineering*, vol. 2015, no. 1, pp. 6–16, 2015.

[15] L. Tagliavini, G. Colucci, A. Botta, P. Cavallone, L. Baglieri, and G. Quaglia, "Wheeled mobile robots: State of the art overview and kinematic comparison among three omnidirectional locomotion strategies," *Journal of Intelligent & Robotic Systems*, vol. 106, no. 3, p. 57, 2022.

[16] M. J. A. Safar, "Holonomic and omnidirectional locomotion systems for wheeled mobile robots: A review," *Jurnal Teknologi*, vol. 77, pp. 91–97, 12 2015.

[17] L. Xie, C. Scheifele, W. Xu, and K. A. Stol, "Heavy-duty omni-directional mecanum-wheeled robot for autonomous navigation: System development and simulation realization," in *2015 IEEE International Conference on Mechatronics (ICM)*, 2015, pp. 256–261.